

INSIGHT FROM FUKUSHIMA DAIICHI UNIT 3 INVESTIGATIONS USING MELCOR

REACTOR SAFETY

KEYWORDS: Fukushima Daiichi NPP Unit 3, severe accident, long-term station blackout

KEVIN R. ROBB,* MATTHEW W. FRANCIS, and LARRY J. OTT

Oak Ridge National Laboratory, 1 Bethel Valley Road, MS-6167, Oak Ridge, Tennessee 37831

Received March 29, 2013

Accepted for Publication May 21, 2013

<http://dx.doi.org/10.13182/NT13-43>

During the emergency response period of the accidents that took place at the Fukushima Daiichi nuclear power plant (NPP) in March of 2011, researchers at Oak Ridge National Laboratory (ORNL) conducted a number of studies using the MELCOR code to help understand what was occurring and what had occurred. During the postaccident period, the U.S. Department of Energy (DOE) and the U.S. Nuclear Regulatory Commission (NRC) jointly sponsored a study of the Fukushima Daiichi NPP accident with collaboration among ORNL, Sandia National Laboratories, and Idaho National Laboratory. The purpose of the study was to

compile relevant data, reconstruct the accident progression using computer codes, assess the codes' predictive capabilities, and identify future data needs. The current paper summarizes some of the early MELCOR simulations and analyses conducted at ORNL of the Fukushima Daiichi NPP Unit 3 (1F3) accident. Extended analysis and discussion of the 1F3 accident are also presented taking into account new knowledge and modeling refinements made since the joint DOE-NRC study.

Note: Some figures in this paper may be in color only in the electronic version.

I. INTRODUCTION

I.A. Background

During the 1975–2000 time frame, Oak Ridge National Laboratory (ORNL) conducted an extensive research program to study boiling water reactor (BWR) accident scenarios and phenomena. During this time, Ott largely developed the BWRSAR code to model the progression of severe BWR accidents.¹ To consolidate severe accident modeling tools, BWRSAR was provided to Sandia National Laboratories (SNL) as input into the initial core model development for MELCOR (middle 1980s). The MELCOR code extended severe accident modeling capabilities to predict the source term from severe accidents.

During the early development of MELCOR, a model for the Peach Bottom nuclear power plant (NPP) was

developed and exercised by researchers at Brookhaven National Laboratory² (late 1980s). Later, Carbajo³ expanded and updated the model to MELCOR v1.8.1. This MELCOR model was then expanded by Dycoda, LLC, updated to MELCOR v1.8.5, and then provided back to ORNL in 2003. Francis then added functions to model additional mitigation measures for long-term station blackouts⁴ (LTSBOs). Note that over the 30 yr of code and model development, short-term station blackout and LTSBO accident scenarios for BWRs with Mark I containments, as well as many other scenarios, were investigated.^{1–8}

Soon after the initiation of the Fukushima Daiichi NPP accident, the U.S. Department of Energy (DOE) set up an emergency response team of subject experts. At that time, the MELCOR model, described in the previous paragraph, was revitalized at ORNL and used in early scoping analyses. Much analysis was based on news reports and on very limited data and used models that were not necessarily reflective of the Fukushima Daiichi NPP Units [Unit 1 (1F1), Unit 2 (1F2), Unit 3 (1F3), Unit 4 (1F4), Unit 5 (1F5), and Unit 6 (1F6)]. In addition,

*E-mail: robbkr@ornl.gov

analyses were performed using bounding assumptions and possibilities.

As an example of one early activity, generic LTSBO sequences were run independently at ORNL by Francis and Ott using the Peach Bottom model and at SNL using its own BWR MELCOR model. These results provided ballpark estimates of the accident sequence timing and were passed to the DOE Science Panel to help inform decision makers. The ORNL results are provided in Table I (Ref. 9). Guided by the sequence timing from the MELCOR results and the information available at the time, Ott and Francis predicted that the accident at 1F3 possibly proceeded to an ex-vessel melt that was quenched by sufficient water in the drywell¹⁰ (DW).

TABLE I
Early Scenario Timing Predictions

Event	Relative Timing (h)
Station blackout loss of all on-site and off-site ac power	0.0
Direct-current power depleted	8.0
Water level reduced to top of active fuel	10.8
First fuel rod gap release	12.4
Core plate failure	16.0
Ex-vessel release ^a	19.8
Hydrogen burns in refueling bay	—

^aEx-vessel release not identified at Fukushima Daiichi NPP. (This note was included with original table.)

Following the emergency response period, the DOE Office of Nuclear Energy (DOE-NE) and U.S. Nuclear Regulatory Commission (NRC) jointly sponsored the “Fukushima Daiichi Accident Study” to collect and document data, reconstruct the accident using computer models, and identify future data needs.¹¹ The kickoff meeting was on June 12, 2011, and the final report was published on July 1, 2012.

During that time frame, a series of reports^{11–20} was released; these reports describe the Fukushima Daiichi NPP accident progression (Table II). Our understanding of the accident continued to evolve as the information was studied, and new information was discovered during the decommissioning work and disseminated. Much information used in the joint DOE-NE/NRC “Fukushima Daiichi Accident Study” was derived from the two reports provided by the Government of Japan to the International Atomic Energy Agency^{12,13} (IAEA) as well as other information available as of approximately January 2012. Additional information concerning the accident progression was disseminated through the Tokyo Electric Power Company (TEPCO) Interim Report,¹⁴ as well as during three technical exchange meetings (October 4, 2011, January 25, 2012, and May 8–9, 2012) attended by a wide range of organizations.

As our understanding of the accident evolved, the analysis and simulation of the accident progression continued to evolve. Early analysis results were made publically available¹² from TEPCO, using MAAP, and from the Japanese Nuclear Energy Safety Organization, using MELCOR. TEPCO later updated its analysis and provided the results in its interim report.¹⁴ For the DOE-NE/NRC “Fukushima Daiichi Accident Study,” the Peach Bottom model at ORNL for MELCOR 1.8.5 (Ref. 21) was modified to reflect 1F3. During the course

TABLE II
Key Reports on Fukushima Daiichi NPP Accident

Publication Date	Reference	Author Organization
June 2011	15	IAEA
June 2011	12	Government of Japan
September 2011	13	Government of Japan
October 2011	16	Japan Nuclear Technology Institute
November 2011	17	Institute of Nuclear Power Operators
December 2011	14	TEPCO
March 2012	18	ANS
March 2012	19	Nuclear and Industrial Safety Agency
July 2012	20	Nuclear Accident Independent Investigation Commission
July 2012	11	DOE-NE/NRC

of the work, a number of key uncertainties, associated with operator actions, event timing, and equipment performance, were identified and presented during the three technical exchange meetings. The ORNL 1F3 results included two detailed simulations and several parametric studies (Ref. 11, Sec. 6) and were accompanied by 1F3 simulation results by SNL using MELCOR (Ref. 11, Sec. 4).

This paper discusses some of the results from the joint DOE-NE/NRC study¹¹ and presents extended analysis of 1F3, taking into account new knowledge obtained and additional modeling modifications made since that study. The results are based on our understanding and modeling of the 1F3 accident as of approximately April 2012.

I.B. Accident Progression, Data, and Observations

The general accident progression and some key details relevant to simulating the accident are summarized as follows. Most of the information can be found in multiple references (see Table II). It is stressed that there are many details that are not discussed here. The amount of elapsed time since reactor shutdown is indicated in braces: {h:min}.

I.B.1. Accident Progression and Operator Actions

At 14:47, on March 11, 2012, {00:00}, 1F3 tripped and shut down due to the Tohoku earthquake. The reactor shut down successfully, and no abnormalities are noted to have occurred. As a result of a loss of off-site power, two emergency diesel generators started. At {00:18} the reactor core isolation cooling system (RCIC) was manually activated and automatically tripped at {00:38} because of high water level in the downcomer. Around {00:51} the tsunami caused a loss of alternating-current (ac) power at 1F3. However, direct-current power from the station batteries remained available.

The RCIC system was manually activated again at {01:16} and later tripped for the final time at {20:49}. During RCIC operation, the RCIC was aligned to take suction from the condensate storage tank (CST). The operators closed the minimum flow line, preventing the pumped liquid from being passed to the suppression chamber (SC). Workers throttled the test line (to the CST) and used the flow controller to adjust the liquid injection into the primary system.²²

The diesel-driven fire pump (DD-FP) was turned on at {21:19} (Ref. 23) and used to run containment sprays.²² From {21:19 to 36:18} and {38:21 to 40:56}, the SC sprays were active, and from {40:52} to around {41:53 to 42:23} the DW sprays were active.²² The DD-FP shut off at {55:28} because of fuel depletion.²³

At {21:48} the high-pressure coolant injection (HPCI) system automatically activated. The HPCI system

was configured and manually controlled in the same fashion as described for the RCIC. The reactor water level measurement was lost at {29:49} because of battery depletion.²² A decision was made to inject water into the primary system using the DD-FP instead of the HPCI (Ref. 22). This decision is described as being based on concerns that the HPCI was no longer injecting water into the primary system [the discharge pressure of the HPCI system approached the reactor pressure vessel (RPV) pressure] and concerns regarding HPCI damage due to the low speed of the steam turbine that drives the HPCI pump.²² In addition, at some point, “the Emergency Countermeasures Headquarters and the Main Control Room instructed all operators to shift to DD-FP for water injection, in the event water injection by the HPCI becomes unstable.”²² The HPCI was manually shut off at {35:55} (Ref. 22).

After the HPCI was shut off, the reactor pressure increased to above the discharge capability of the DD-FP before the switchover could occur. Around this time, actuation of the safety relief valves (SRVs) was attempted in order to lower the RPV pressure below the discharge pressure of the DD-FP; however, the SRVs did not actuate. Thus, the capability to inject water into the RPV was lost. Efforts were made to restart RCIC but were unsuccessful. During the RCIC restoration effort, operators passed through the HPCI room. No abnormalities in the HPCI room were noted,²² that is, no steam-filled room or large leakage.

The vent line valve lineup from the SC to the stack was complete at {41:54} with the rupture disk preventing venting. Power was not available to manually actuate the SRVs to depressurize the RPV. As most available batteries were being used in 1F1 and 1F2, workers removed batteries from cars, carried them to the control room, and connected them to the instrument panel.¹³ The RPV is believed to have been depressurized by operators manually actuating an SRV at around {42:21} (Refs. 13 and 16). Based on the DW pressure data, the containment is believed to have successfully vented sometime between {42:23} and {42:37}. As the rupture disk was preventing venting, the depressurization of the RPV likely increased the containment pressure enough to fail the rupture disk. At {44:30} it was confirmed the vent line was closed; it reopened at {45:43} after gas cylinders were replaced. Because of difficulties in maintaining the vent line valves open, the vent line intermittently closed and opened over the next couple of days.

After the RPV was depressurized, freshwater injection into the primary system via a fire engine started at {42:38} and lasted until the freshwater source was depleted at {45:33}. The fire engine switched over to a different water source, and seawater injection commenced {46:25 to 58:23}. The DD-FP is noted to have been operating during the switchover {45:33 to 46:25}; however, it is unclear whether the DD-FP was injecting

water into the primary system during that period. Owing to the decreasing water level of the backwash valve pit (seawater source), water injection was temporarily suspended {58:23 to 60:33} while the fire engine was repositioned. Seawater injection then recommenced at {60:33}. At {68:14} water injection ceased because of damage caused by the 1F3 reactor building explosion. Seawater injection resumed at {73:43} and continued through and beyond the explosion of the 1F4 reactor building at {87:13}.

I.B.2. Summary of Periods of No Water Injection

The 1F3 accident followed a LTSBO scenario. Many previous BWR LTSBO analyses assume battery failure and loss of cooling functions in <8 h after reactor shutdown (Ref. 2, 6 h; Ref. 6, 6 h; Ref. 24, 4 h). However, for 1F3, the RCIC was used to successfully manage the reactor decay heat for 20 h and 49 min. After the RCIC shutdown, there was a 59-min delay until the HPCI started. The delay is minor given that it would take a few hours for the core to uncover at that point. The HPCI was then used to successfully manage the decay heat until at least 29 h and 49 min into the accident, when liquid level indication was lost as a result of battery depletion. Between {29:49} and {35:55}, it is uncertain whether the HPCI was successfully injecting water into the reactor to offset the decay heat. After HPCI shutdown, it appears there were four major periods of no water injection. The causes for these periods are noted in Sec. I.B.1. The seven periods of time during which water was

not being injected into the primary system are summarized in Table III.

I.B.3. Data for Simulation Comparisons

The publicly available data provided by TEPCO for the RPV, DW, and SC pressure and the RPV water level²⁵ are used for comparison. These data are contained within the data portal developed by Idaho National Laboratory as part of the joint DOE-NE/NRC “Fukushima Daiichi Accident Study.”¹¹ Note that there are time frames in which data are unavailable. This is especially true for the RPV temperature data, which begin at 6:30 A.M. on March 19, 2011 (Ref. 26). There are also questions concerning the validity and uncertainty of the data.

There are two other data sources that are not included in the comparison. First, data in the form of strip-chart recordings for the RPV pressure, in addition to other parameters, have been released by TEPCO. Much of the data are limited to the first 1.5 h; however, some data, such as the RPV pressure, are provided up to 40 h after accident initiation. The translation, digitization, and verification of the strip-chart data are currently not publicly available.

During the ongoing decommissioning work, additional data have been taken, and observations have been made by TEPCO. A number of surveys have mapped the dosage inside the reactor building. A door to the room containing the SC torus (torus room) in the northeast corner was found to be bowed outward (outward from the direction of containment) on March 14, 2012 (Ref. 27). During an inspection on May 23, 2012, the door to the

TABLE III
Time Periods of No Water Injection into RPV

Period	Time ({h:min} to {h:min})	Duration (min)	Timeline Period (Between)
1	00:00 to 00:18	18	Reactor scram RCIC startup—start of cooling water injection
2	00:38 to 01:16	38	RCIC shutdown—stop of cooling water injection RCIC startup—start of cooling water injection
3	20:49 to 21:48	59	RCIC shutdown—stop of cooling water injection HPCI startup—start of cooling water injection
4 ^a	35:55 to 42:38	386	HPCI shutdown—stop of cooling water injection Fire engine injection start—freshwater source
5 ^b	45:33 to 46:25	52	Fire engine injection stop—freshwater source Fire engine injection start—seawater source
6	58:23 to 60:33	130	Fire engine injection stop—seawater source Fire engine injection start—seawater source
7	68:14 to 73:43	329	Fire engine injection stop—seawater source Fire engine injection start—seawater source

^aHPCI may have started injecting little or no water before {35:55}.

^bDD-FP was possibly injecting water during this time.

traversing in-core probe room (TIP room) was observed to be on the ground and was described as being blown outward.²⁸ Inspection of the torus room on June 6, 2012, indicated the torus room and nearby stairwell were partially filled with water up to approximately the midpoint of the SC (Ref. 29). Future examination of these observations may provide additional insight concerning the accident progression.

II. MELCOR MODELING OF 1F3

II.A. Model Overview

Both Peach Bottom (Units 2 and 3) and 1F3 are BWR/4 series reactors with Mark I containments. 1F3 is a slightly smaller reactor containing 548 fuel assemblies compared to the 764 assemblies in Peach Bottom.

The MELCOR model of Peach Bottom, described in Sec. I.A, was used as the basis for the 1F3 model. The Peach Bottom model was modified to reflect the systems and the accident progression at 1F3. The model has been previously described in detail.¹¹ In summary, RPV volumes and masses, DW volume, SC and CST volume and initial water mass, core decay power and fuel loading, SRV setpoints, and flow rate capacity for the HPCI and RCIC were modified to reflect 1F3. A schematic of the system nodalization is provided (Fig. 1, adapted from Ref. 4) as well as a schematic of the core nodalization [Fig. 2 (Ref. 4)].

The timeline events, including reactor shutdown timing, loss of ac power, RCIC and HPCI availability, SC venting availability, operator action to depressurize the RPV, and the timing and flow rate of the fire injection line, were prescribed to the model (Table IV). Additional logic in the model, controlling the RCIC and HPCI flows

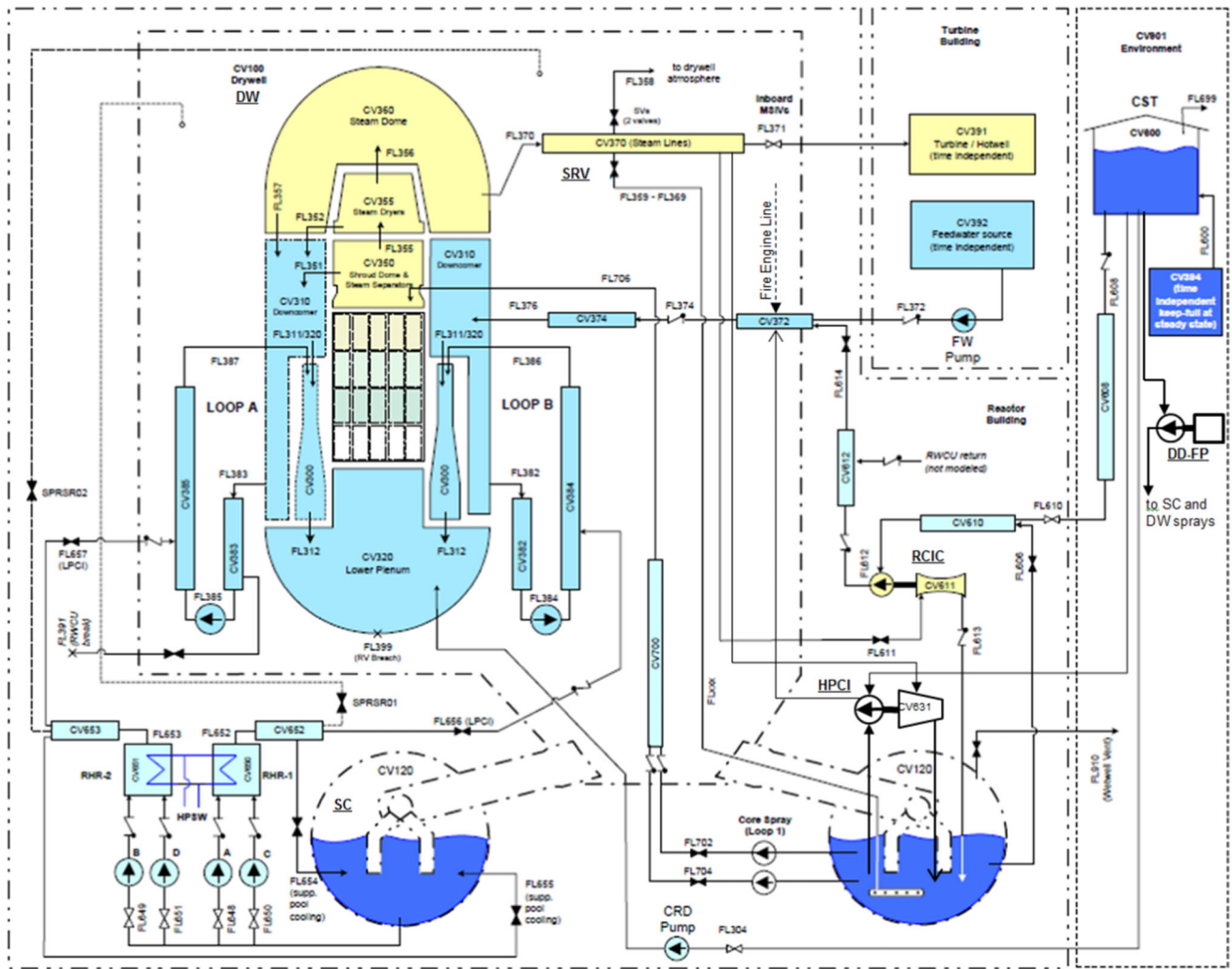


Fig. 1. Reactor coolant system schematic as modeled for 1F3.

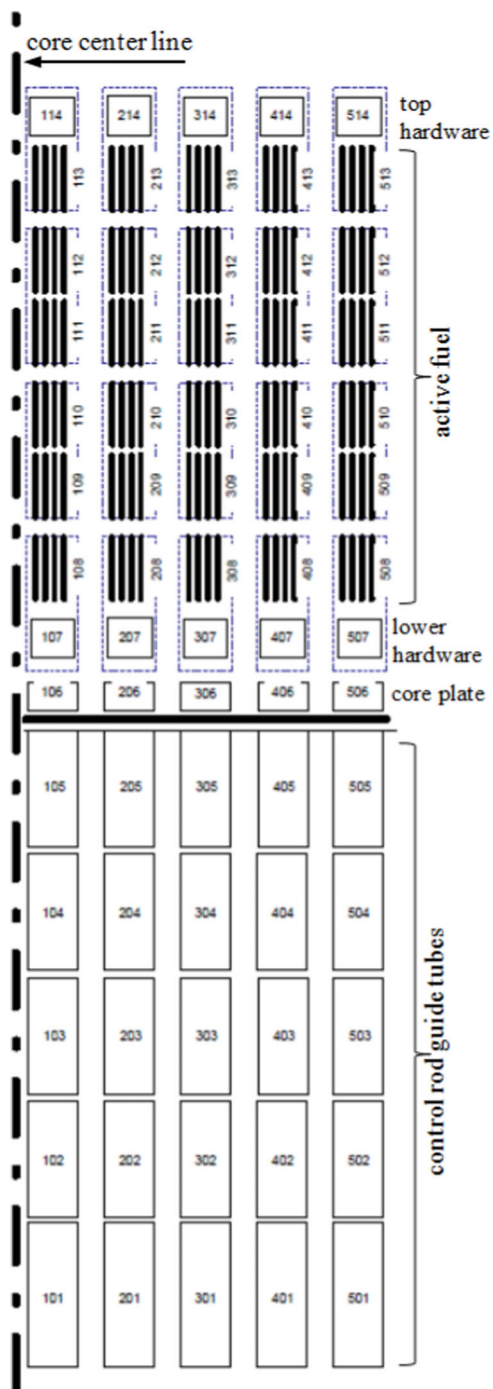


Fig. 2. Core nodalization for 1F3.

through the minimum flow and system test line, was added and modified. Likewise, a flow path and timing for water injection from the fire engines were added.

Sections II.A.1, II.A.2, and II.A.3 highlight some of the modifications made to the model for use in the joint DOE-NE/NRC “Fukushima Daiichi Accident Study.”¹¹ Section II.B discusses additional modifications made

TABLE IV
Applied Timeline Summary

Time	Event
00:00	SCRAM
00:18	RCIC available
00:38	RCIC unavailable
00:51	Alternating-current power lost
01:16	RCIC available
20:49	RCIC unavailable
21:19	Suppression chamber sprays start
21:48	HPCI starts
29:00	HPCI liquid injection stops (assumed)
35:55	HPCI shuts down; steam flow stops
36:18	Suppression chamber sprays stop
38:21	Suppression chamber sprays start
40:52	Drywell sprays start
40:56	Suppression chamber sprays stop
41:54	Vent lineup complete with rupture disk intact (closed)
42:08	Drywell sprays stop
42:21	SRV opens; RPV is depressurized
42:38	Fire engine water injection RPV starts
44:30	Vent line closes
45:33	Fire engine water injection RPV stops
45:43	Vent line opens
46:25	Fire engine water injection RPV starts

since the “Fukushima Daiichi Accident Study.” Finally, Section II.C notes some of the model deficiencies.

II.A.1. SRV Actuation

In the original, unmodified Peach Bottom MELCOR model, the logic for automatic SRV actuation relied upon the differential pressure between the main steam line and the SC. However, while the reactor pressure is high, the SRV actuates at a predefined main steam line pressure setpoint and does not depend upon the differential pressure. This was corrected for the 1F3 model.

II.A.2. Suppression Chamber Nodalization

In the unmodified Peach Bottom MELCOR model, the SC was modeled using a single control volume. Modeling the SC in this fashion is common.²⁴ However,

modeling the torus in this fashion cannot capture localized saturation and thermal stratification that may occur in the SC (Ref. 30). As a stopgap measure, the torus was divided into eight sections in the circumferential direction as described in Ref. 11. This remains as an area for future model refinement and analysis.

II.A.3. Fire Engine Water Injection

The water injection into the primary system RPV from the fire engines was prescribed to the model, and the details are summarized in Table V. The water injection timing is based on the timeline presented in Refs. 13 and 22. Using this timing, the water flow rate was determined using estimates of the total water injection volume from TEPCO (Ref. 31). The amount of water that was injected and made its way to the core region is currently a key uncertainty. In addition, the possible usage of the DD-FP to inject water after RPV depressurization is unknown to us.

II.B. Model Modifications

A few modifications have been made to the 1F3 model since the joint DOE-NE/NRC “Fukushima Daiichi Accident Study.”¹¹

II.B.1. Decay Heat

The model previously used the decay heat based on ANSI/ANS-5.1-1979 (Ref. 32), the American Nuclear Society (ANS) American National Standard for light water reactors. TEPCO has provided decay heat data,¹¹ for specific points in time, based on isotope depletion and decay calculations from the ORIGEN-2 code.³³ This decay heat was ~5% lower than the ANSI/ANS-5.1-1979 decay heat curve. Additional data points were

estimated between the TEPCO data points through fitting the ANSI/ANS-5.1-1979 decay heat curve to the TEPCO data. These additional points were implemented to reduce the error introduced through MELCOR’s interpolation (see Sec. IV.A.1, Signature 1).

II.B.2. HPCI Model

We investigated a few methods of modeling the HPCI, each including several cases, to capture the impact of uncertainty in the HPCI performance and operator actions. This included modeling the flow rates as a function of the main steam line to SC differential pressure, assuming various values for operator throttling, simulating system degradation with assumed pump/turbine curves, and fixing the flow rates. Uncertainties in the off-nominal performance of the HPCI system, coupled with the lack of detailed descriptions of operator actions (as a function of time) and RPV water level and SC pressure data, complicate modeling the actual HPCI performance.

For the current study, the liquid injection rate into the feedwater line and the steam flow rate through the HPCI turbine were specified, a posteriori (Fig. 3). The purpose was to identify the flow rates needed to reproduce the available reactor pressure and two-phase water level data. It is assumed that using the flow controller and throttling the test line result in this HPCI performance. The pumped liquid flow was suctioned from the CST and injected into a feedwater line. The HPCI steam turbine, powering the HPCI pump, was supplied steam from the main steam line and vented the condensing steam into the SC.

The sparse primary system to containment differential pressure data, derived from Ref. 25, is provided in Fig. 4. The TEPCO data indicate that the differential pressure between the main steam line and the containment fell to

TABLE V
Assumed Water Injection Timing and Rate via the Fire Engines into RPV

Day	Water Injection Timing ({h:min} to {h:min})	Duration (min)	Injection Rate (kg/s)
March 13	42:38 to 45:33	175	7.88
	45:33 to 46:25	52	0
	46:25 to 57:13	648	7.88
March 14	57:13 to 58:23	70	5.41
	58:23 to 60:33	130	0
	60:33 to 68:14	461	5.41
	68:14 to 73:43	329	0
	73:43 to 81:13	450	5.41
March 15	81:13 to —	—	8.94

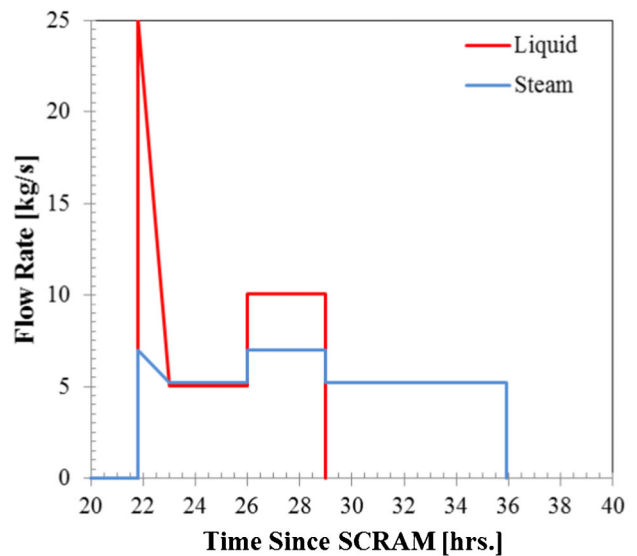


Fig. 3. Assumed HPCI steam draw and liquid injection rates.

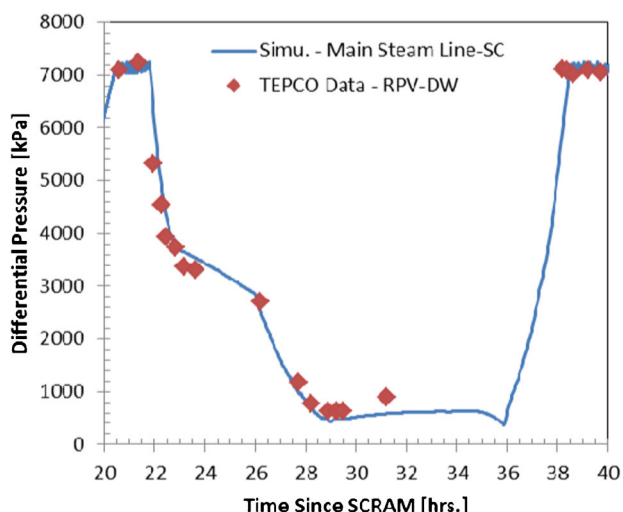


Fig. 4. Main steam line to DW differential pressure data and prediction.

631 to 901 kPa (92 to 131 psi) starting at {28:13} (Fig. 4) and that the main steam line pressure remained low within the {28:13} to {36:13} time frame.²⁵ Although there are gaps in the containment pressure data, the differential pressure likely remained low until the HPCI was shut off at {35:55}. For the model, it was assumed the HPCI pump was no longer injecting water into the primary system after {29:00}. The ability of the HPCI to inject water and provide cooling water to the bearings (~4 kg/s) under the conditions of low reactor pressure and low differential pressure driving the turbine is currently unclear to us. HPCI modeling remains a key area for future modeling effort and refinement.

II.B.3. Containment Sprays

Early reports did not describe containment spray usage.^{12,13} Spray usage was previously assumed by us for

the ORNL 1F3 analyses presented in the joint DOE-NE/NRC “Fukushima Daiichi Accident Study.”¹¹ This assumption was based on information contained in the English translation of the operator logbook such as the discharge pressure of the DD-FP and the diesel fuel level.²³ TEPCO indicated that containment sprays were used in the interim reports^{14,22}; however, the flow rate remains unknown. A rough analysis by us based on the fuel consumption rate of the DD-FP and the required head suggests the DD-FP may have the capability to inject ~3 to 10 m³/min of water.¹¹ Table VI provides the containment spray timing and the assumed flow rate used in the current and previous¹¹ analyses. The current work assumes the DW sprays shut off at {42:08}, the midpoint in the range provided by TEPCO; see Table VI.

II.C. Model Limitations

The containment volumes and elevations are representative of 1F3. However, the elevations/heights of the vessels, piping, and building were not modified. A limited comparison between information for some components of 1F3 and the MELCOR model showed the relative elevations were comparable.

Specific failure modes, such as head lifting, are modeled generically without taking reactor-specific information into account. More detailed information, such as the containment head flange geometry, the size and pretension of the bolts, and other penetration details, is required to develop accurate models of the containment failure modes.

The modeling of the reactor building (outside of containment) was not modified to reflect the Fukushima Daiichi NPP. Resources were focused on modeling the in-containment features and accident progression. Previous work notes the complexities in reactor building modeling and indicates that the building can have an important impact on mitigating radionuclide releases.³⁴ More

TABLE VI
Containment Spray Details

Spray Location	TEPCO Information ^{14,22}	Previous Study ¹¹		This Study	
	Timing	Timing	Flow Rate	Timing	Flow Rate
Suppression chamber	{21:19} to {36:18}	{21:19} to {36:18}	25.24 ℓ/s	{21:19} to {36:18}	12.62 ℓ/s
Suppression chamber	{38:21} to {40:56}	{38:21} to {40:56}	25.24 ℓ/s	{38:21} to {40:56}	6.31 ℓ/s
Drywell	{40:52} to {41:53 to 42:23}	{40:52} to {54:28}	25.24 ℓ/s	{40:52} to {42:08}	6.31 ℓ/s

information and effort are required to accurately model the room volumes, elevations, and flow paths, including the ventilation system.

The vent lines are not modeled in detail. Instead, a flow path is specified that takes fluid from containment directly to the outside environment (or other specified location). This rough modeling approach to venting does not capture cross-flow to 1F4, radionuclide deposition onto the walls of the vent pipe, the trapping of gases between segments, or the hydraulics of the vent lines.

Because of the MELCOR model limitations mentioned, the study focuses on the in-containment accident progression.

III. SIMULATION RESULTS AND ANALYSES

The simulation predictions are compared with the available data from TEPCO for the first 48 h of the accident in Figs. 4 through 12. The results are discussed within three time frames.

III.A. SCRAM to HPCI Startup, {0:00} to {21:48}

The reactor pressure and water level are fairly well reproduced (Figs. 6 and 7). The “sawtooth” reactor pressure and water level during RCIC operation are artifacts of the RCIC modeling methodology. However, the overall water injected and steam vented from the reactor to the SC are judged to be comparable.

The containment pressure is underpredicted (Fig. 8). We believe this is due to the modeling of the SC, which can only approximately capture localized saturation and cannot capture thermal stratification and convection cell

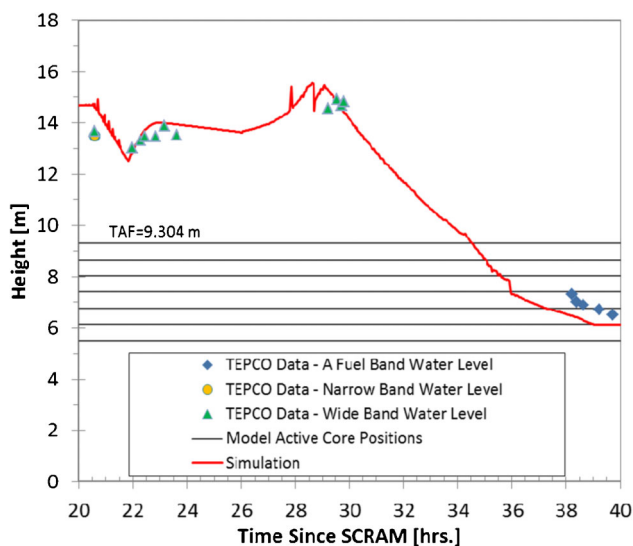


Fig. 5. Reactor two-phase water level data and prediction.

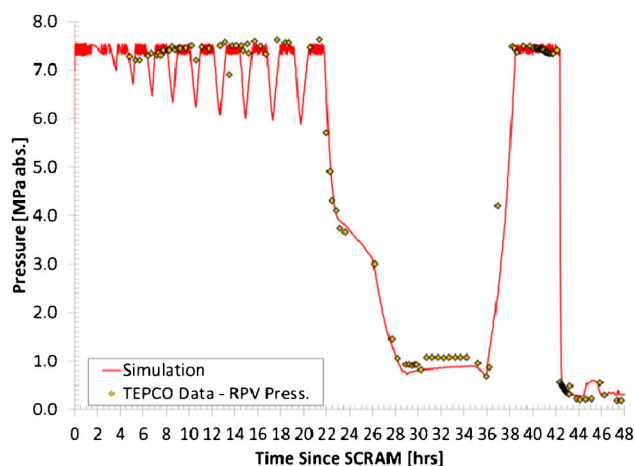


Fig. 6. Pressure in RPV.

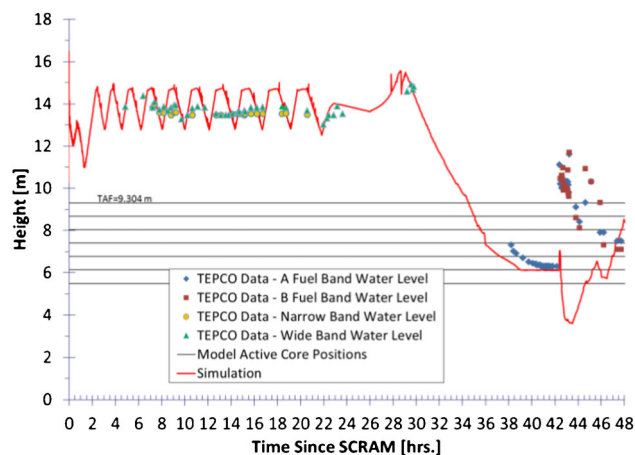


Fig. 7. Water level in core region.

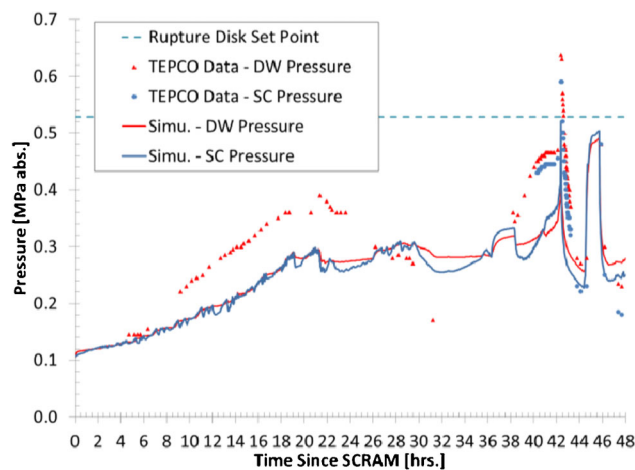


Fig. 8. Pressure in containment.

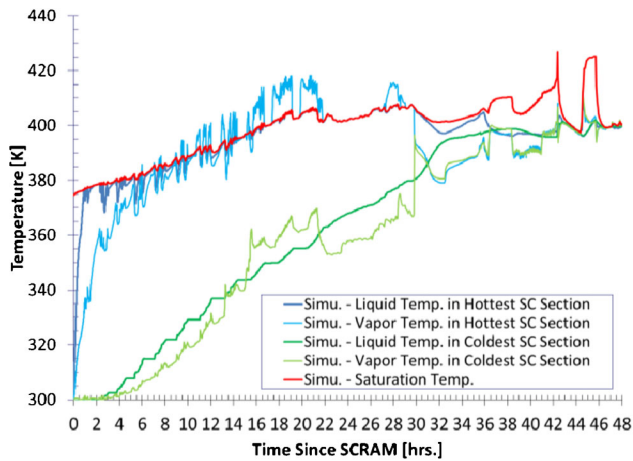


Fig. 9. Suppression chamber temperatures.

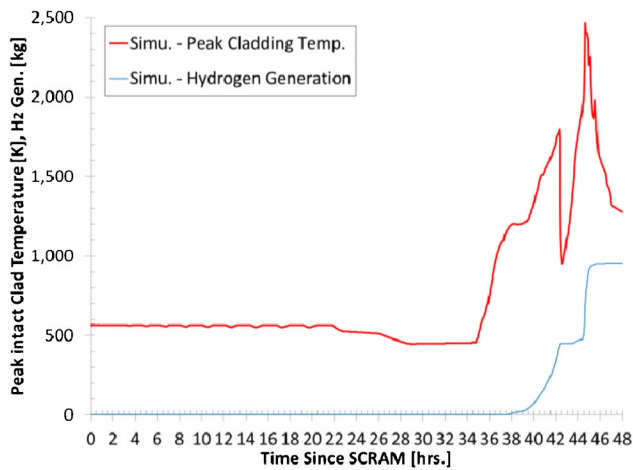


Fig. 10. Peak clad temperature and hydrogen generation.

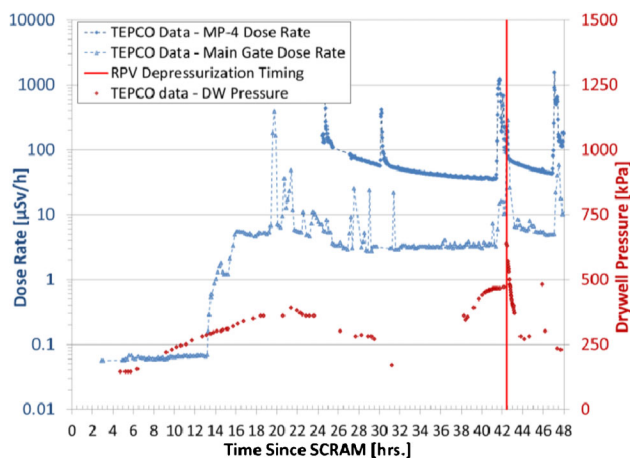


Fig. 11. Dose data³⁵ at main gate and MP-4.

phenomena. With the current SC nodalization (eight control volumes), the section where the steam is vented saturates in 50 min, whereas the coldest section (180 deg opposite) saturates >40 h later (Fig. 9). Based on previous work, when the SC is modeled as one large control volume, it takes tens of hours for the SC to saturate.¹¹ Another possible cause for the discrepancy in containment pressure is flashing of water leakage through the recirculation pump seals, which is assumed to be zero in the current simulation.

III.B. HPCI Startup to RPV Depressurization, {21:48} to {42:21}

As discussed in Sec. II.B.2., the HPCI performance was specified to reproduce the available reactor pressure and water level data. As a result of specifying the HPCI flow rates (Fig. 3), the reactor pressure (Fig. 6) and two-phase water level (Figs. 5 and 7) are well reproduced.

After the HPCI steam flow shuts off at {35:55}, the primary system is predicted to repressurize in 153 min. This prediction is in contrast to the TEPCO data, which indicate the system repressurized within 62 to 138 min (Ref. 25), and strip-chart data released by TEPCO, which suggest ~100 min. A number of factors influence the repressurization rate, including the reactor water level, power, mass, and volume. If the reactor mass, volume, and power are accurately modeled, then the repressurization rate can be used to “back out” the reactor water level. Based on a number of previous simulations, the repressurization period extends with higher initial water level. The simulation results suggest the two-phase water level was at or below the top of active fuel (TAF) when the HPCI shut off at {35:55}, supporting the notion that the HPCI water injection was not effectively offsetting the decay heat.

The containment pressurization (Fig. 8), with data starting at {38:13}, can also provide a number of insights. At {38:21} the SC sprays are activated. Both the data and simulation exhibit an ~150-kPa drop in the DW pressure around this time. Despite the use of containment sprays and nearly an additional 20 h for decay heat reduction, the containment pressurization rate based on the TEPCO data (~49 kPa/h) from {38:23} to {40:43} is more than double the containment pressurization rate during the first 18 h (~20 kPa/h). The additional heat and noncondensable gas generation from cladding oxidation during this period could be a cause for the high containment pressurization rate from {38:23} to {40:43}. Despite the simulation predicting cladding oxidation starting at {37:20}, with first gap releases occurring at {37:45}, the containment pressurization is underpredicted during this period. This suggests the current simulation may be underpredicting the amount of cladding oxidation occurring during this time period. Uncertainties related to the containment spray modeling (flow rate, efficiency) may also contribute to the discrepancy.

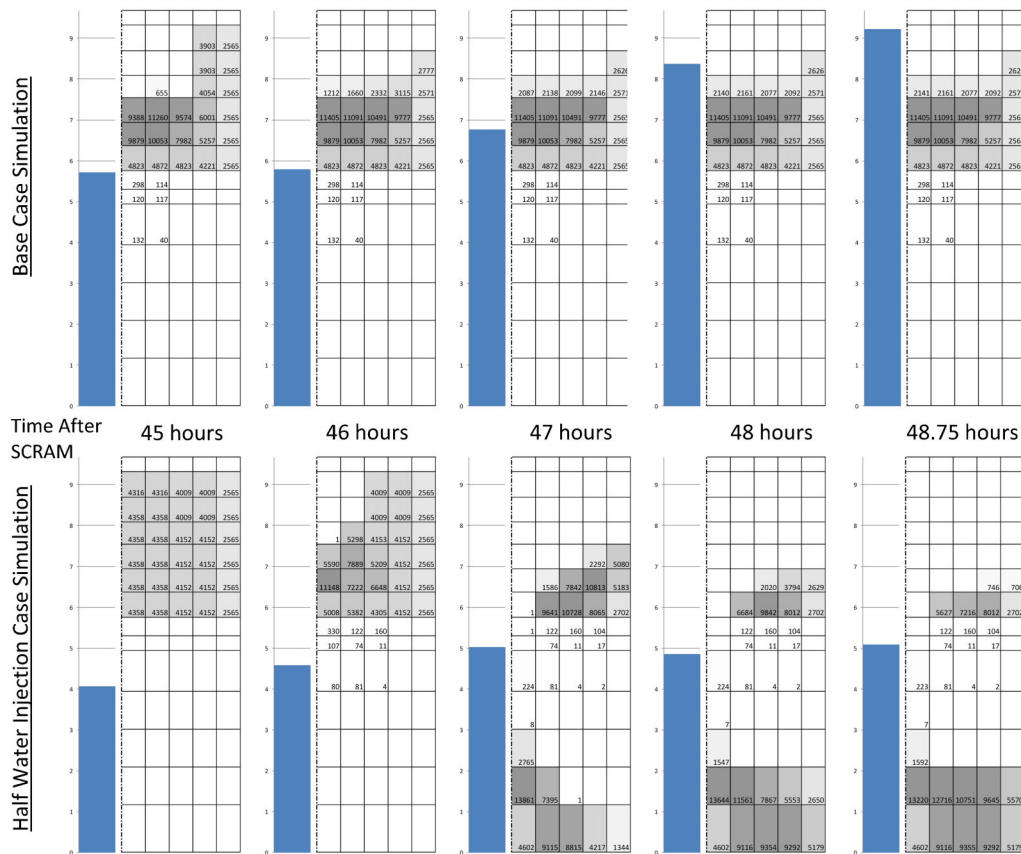


Fig. 12. Fuel location (kg) and two-phase water level (m) versus time; see Fig. 2 for nodalization.

From {40:43} to {42:08}, the TEPCO data indicate the DW pressure plateaued to ~465 kPa absolute (abs) (67.4 psia) (Fig. 8). It is unclear why the pressure plateaued. In contrast, the simulation predicts a continued increase in containment pressure. One possible cause for the pressure plateau is that the containment could have begun leaking at this pressure. This possibility may be supported by the radiation measurements at the main gate and monitoring point 4 (MP-4), which indicate increased activity around {41:30}, which is ~50 min before containment venting is noted to occur. This is shown in Fig. 11 by the increased magnitude of the dose rate data points just before the indicated vent timing. Another possibility is that the containment spray flow rate was increased during this period, increasing containment cooling and condensation.

**III.C. RPV and Primary Containment Vessel
Depressurization and Beyond, {42:21} to {49:00}**

The RPV is depressurized at {42:21} in the simulation by activating five SRVs with the automatic depressurization system, which causes a spike in the containment pressure (Fig. 8). Although the predicted containment pressure is less than the data indicate, the

spike in containment pressure is still large enough to cause the rupture disk to fail and open the vent line. The RPV depressurization causes the water level to drop well below the core in the simulation (Fig. 7). However, the data suggest the water level was higher after containment venting. We believe the water level measurements after RPV venting are not accurate, possibly because of flashing or gas entering the measurement reference leg. The lower saturation temperature results in a predicted decrease in cladding temperature (Fig. 10). In addition, the reduced steam flow through the core reduces the cladding oxidation rate temporarily until approximately {44:30} (Fig. 10).

Water injection starts soon after venting at {42:38}. The simulation predicts that considerable core damage occurs before the assumed water injection timing and rate are able to offset the decay heat and reflood the core. Most fuel relocation is predicted to occur around {44:40} to {45:38}. By the end of the simulation, approximately two-thirds of the fuel cladding has melted and relocated. The core degradation progression is illustrated in Fig. 12 with respect to the core nodalization depicted in Fig. 2.

The water injection rates remain a key uncertainty. TEPCO has provided estimates of the amount of water injected; however, the amount of uncertainty is unknown.

In addition, the flow rate as a function of time is unknown. Valve misalignments or leaks in the piping, connections, and valves provide additional uncertainties. An additional simulation was run in which half of the assumed water injection (Table V) is supplied to the core (Figs. 12, 13, and 14). As expected, much more core damage occurs. However, interestingly, the decreased water addition results in starving the cladding of steam, which delays the cladding heatup and reduces cladding oxidation and hydrogen generation (Fig. 13).

Beyond 48 h, the accident progression is primarily dependent upon the rate at which water is injected into the core region. The vent timing has a secondary impact by varying the containment and RPV pressure and therefore the saturation temperature. The current simulation predicts

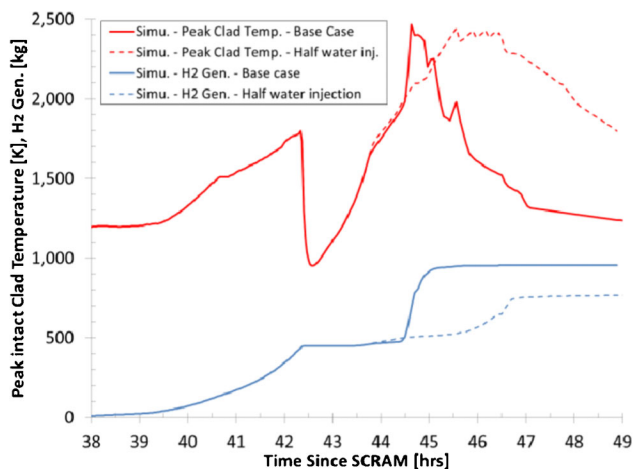


Fig. 13. Predicted peak cladding temperature and hydrogen generation.

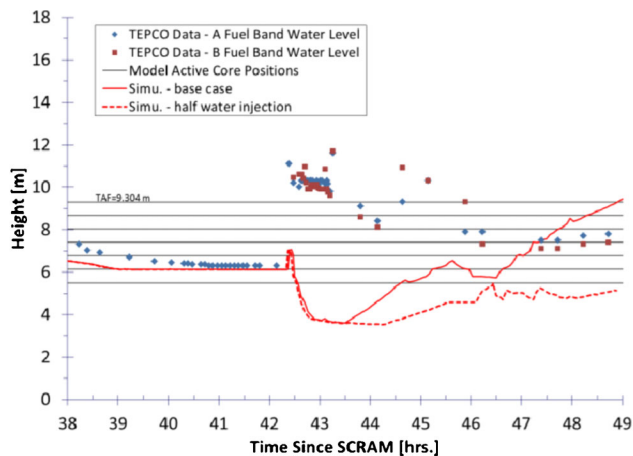


Fig. 14. Water level comparison assuming decreased water injection from fire engine.

that sufficient hydrogen is generated for explosions in the 1F3 and 1F4 reactor buildings.

IV. INSIGHT AND RECOMMENDATIONS

IV.A. Signatures

Sections IV.A.1 through IV.A.6 describe some explanations for behaviors that can be observed in the simulation results. These are provided to aid modelers and those trying to understand modeling methodologies and results.

IV.A.1. Signature 1: Rapid RPV Water Level Drop

After reactor shutdown, there is a rapid drop in the RPV water level due to void collapse followed by a relatively high boiloff rate from the initially high decay heat. If the RCIC is not activated, the water level will reach TAF around {1:15} to {1:30}. The following should be taken into consideration to accurately model this time regime.

First, care must be taken to ensure the model has converged to the correct initial RPV void at the time of reactor shutdown.

Second, TEPCO indicates the RCIC was manually activated at {0:18} and automatically tripped at {0:38} because of high water level. If the RCIC is not activated during this time, the water level will continue to fall and will be near TAF when the RCIC is said to be manually restarted at {1:16}.

Third, TEPCO provided six decay heat data points for the first 3 h after SCRAM. If these data are directly implemented into MELCOR, the decay heat is over-estimated by ~5% owing to the linear interpolation of the data in MELCOR. The higher decay heat results in a higher boiloff rate of the water in the reactor core. This water is replenished by the RCIC from the CST. The increased water injection by the RCIC into the reactor to offset the higher decay heat results in more rapid depletion of the CST.

To decrease the error introduced by the linear interpolation of decay heat data in MELCOR, an additional ten data points were interpolated and incorporated into the current model. The additional data points were determined by first shifting the ANSI/ANS-5.1-1979 decay heat curve³² such that it overlaid the decay heat data points TEPCO provided and then using the curve to guide the selection of the additional data points.

IV.A.2. Signature 2: Increasing RPV Pressure

If the modification to the modeling of the SRV logic is not made (Sec. II.A.1), the actuation point of the SRV will increase with increasing containment pressure. Thus, once the RPV reaches the lowest SRV setpoint, the RPV pressure will increase at approximately the same rate as containment pressure. This can be easily observed as an increasing reactor pressure over the time period of RCIC

operation. The increased pressure at which the steam is being vented increases the internal energy of the vented steam, reducing the amount of steam that needs to be vented. Note that underprediction of the containment pressurization, perhaps due to deficiencies in the SC modeling, can mask this effect.

IV.A.3. Signature 3: Slow Containment Pressurization

The current and previous^{11,12} simulations underpredict the pressurization of the containment during RCIC operation. Several modeling assumptions and code issues have been identified as possible contributors to the decreased pressurization rate. We believe the primary cause for the discrepancy in the current simulation results is the first two issues discussed.

First, if steam is vented through one location in the SC for extended periods, local saturation and thermal stratification can occur. Modeling the SC using one control volume in MELCOR cannot capture these effects as well as other thermal-hydraulic phenomena such as local and global recirculation cell formation. The current model simulates the SC using eight control volumes (divided in the circumferential direction). This allows for energy to be deposited into a section of the pool, for example, venting from a single SRV, instead of the whole pool. The simulation predicts that one section of the pool saturates within 1 h of the accident, whereas it takes >40 h for the coolest section to saturate (Fig. 9). However, this nodalization cannot capture convection cells or thermal stratification within a section. Local saturation, stratification, and recirculation phenomena were previously investigated,³⁰ and it is possible these may have occurred in the 1F3 SC.

Second, the condensation of submerged/rising steam bubbles in a pool is modeled in MELCOR using the product of two empirical efficiencies. The first efficiency accounts for the bubble rise distance. The second efficiency accounts for the water subcooling. The product of the two efficiencies determines the fraction of steam condensed in the pool versus passed through the pool to the atmosphere. The containment pressurization is impacted by the amount of steam that is vented into the SC and not condensed. For the current simulations, the default values for the efficiencies were used. However, the pool subcooling efficiency was modified in previous simulations using a user-defined option in MELCOR (Ref. 11, Sec. 6). The water subcooling efficiency was set to 100% for pool subcooling of 6 K instead of the default 5 K. This had a noticeable impact on the containment pressurization and aided reproduction of the TEPCO containment pressure data. Note that modeling deficiencies in capturing localized saturation (see previous paragraph) also impact the predicted steam condensation by the pool.

Third, the recirculation pump seals can degrade and leak if they are not cooled. Modeling leakage of

high-temperature steam into containment increases the containment pressurization rate. However, as the recirculation pumps were not in operation during the accident, it is unclear whether the seals were actually compromised, resulting in significant leakage.

Fourth, if the RCIC is modeled as bypassing flow into the SC (through the minimum flow line), the subcooled water will decrease the containment pressurization. The RCIC should not be modeled in this fashion, as the operators are described as having closed the minimum flow line (to the SC) and instead used the system test line (to the CST) (Ref. 22). This same comment applies to the HPCI.

Finally, overprediction of steam condensation in the DW or underprediction of the heat transfer from the reactor primary system to the DW may also result in an underprediction in the containment pressurization.

IV.A.4. Signature 4: "Sawtooth" Reactor Pressure

As noted in Sec. III.A, the predicted "sawtooth," up-down-up-down reactor pressure during RCIC operation is due to the intermittent injection of water into the RPV. Operators actually throttled the RCIC to smooth out and reduce such variations. This manner of operation is supported by the strip-chart RPV pressure data released by TEPCO. Additional modeling effort is required to correct this. However, this modeling detail likely has little impact on the overall accident progression, as the RCIC was able to successfully offset the decay heat.

IV.A.5. Signature 5: Long RPV Repressurization

As discussed in Sec. III.B, the RPV repressurization (Fig. 6), starting after the HPCI was shut down at {35:55}, gives an indication of the water level at {35:55}. Very long repressurization times (a few hours) can be the result of initially high (above TAF) water levels at {35:55}. Other modeling factors that can influence this include low decay heat and excessive reactor mass or primary system volume.

IV.A.6. Signature 6: Early-Late Depressurization

The timing of containment depressurization around {42:21} can be impacted by the modeling approach. In the current model, the vent line is available at {41:54}, after which time the vent line will open once the containment pressure surpasses the rupture disk setpoint (528 kPa abs). Modeling the vent line in this fashion, instead of specifying a time when the vent line opens, can result in venting occurring any time after {41:54} instead of when venting was noted to occur.

IV.B. Simulation Results Summary

The simulation results suggest the RCIC at 1F3 was able to successfully manage the decay heat until it shut off

at {20:49}. The containment pressure underprediction is attributed to deficiencies in modeling the SC and/or recirculation pump seal leakage.

Stemming from uncertainties in the HPCI performance, the HPCI liquid and steam flow rates were specified a posteriori in this investigation. The purpose was to provide insight into the flow rates that could reproduce the existing reactor pressure and water level data. The HPCI system is rated for 268 kg/s of injection capability.¹² For the Hatch NPP, the steam requirements while the HPCI is injecting 268 kg/s and is suctioning from the CST range from 13.8 to 23.7 kg/s, depending on the reactor and SC pressures. The values for the water injection and steam flow used in the simulation in order to reproduce the reactor pressure and water level are ~2% to 10% and 22% to 51% of these nominal system values for the liquid and steam flow, respectively (Fig. 3). However, the HPCI was not operating under nominal conditions.

The HPCI likely managed the decay heat until {29:49}; however, after this, the HPCI may have not been able to offset the decay heat. A water level below TAF (Fig. 5) at {35:55} is supported by this and previous simulations that we performed comparing the predicted time it took to repressurize the RPV after {35:55} and the data (Fig. 6). This also provides credibility to the water level measurement data from {38:14} to {42:09}, which indicate the water level was below TAF. Furthermore, the containment pressurization rate from {38:23} to {40:43} (Fig. 8) suggests cladding oxidation was occurring during this time. Finally, one possible explanation for the increased radiation activity around the main gate at {41:15} (Fig. 11) could be from cladding failure (occurring before {41:15}) and containment leakage, possibly supported by the plateau in containment pressure data (Fig. 8), prior to the venting that occurred around {42:21}.

Using the water injection estimate information from TEPCO, simulations^{11,12} generally predict limited core degradation that is later quenched in-vessel. However, the amount of water that made its way to the core region remains a key uncertainty. Decreasing the water injection by half resulted in large-scale core relocation before the end of the simulation. If that simulation were extended, failure of the lower head and melt relocation would likely be predicted.

As noted earlier, because of limitations in time and available information, the simulation does not have 1F3-specific models for predicting containment leakage or accurate reactor building modeling outside containment. This deficiency limits the use of the model in predicting radionuclide and hydrogen transport out of containment.

IV.C. Areas Recommended for Future Work and Consideration

From early in the accident through now, our knowledge of the accident has continued to evolve. Like our understanding, the models and tools used for analysis

have also continued to evolve. As more data are obtained during the cleanup and decommissioning of 1F3, it is anticipated that some of the insight and conclusions in this paper should be revisited and further refined.

Modeling of the ability of the suppression pool to condense steam released through an SRV for an extended period of time needs to be revised in the MELCOR model. The one-control-volume approach used in past and recent simulation work as well as the eight-control-volume approach used in this study both inadequately capture the SC thermal-hydraulic phenomena and resulting containment pressure response seen in 1F3. This may require that enhanced modeling of two-phase and convection phenomena be incorporated into MELCOR.

The performance of the HPCI is key in predicting and understanding the possibility for core degradation early {29:49 to 42:38} in the accident. Additional analysis of the available data during this period, and higher-fidelity modeling of the HPCI system, may prove fruitful.

The water injection details (timing and rate) by the fire engines, and possibly the DD-FP, remain as a key uncertainty. Higher-fidelity modeling of the fire engine pumps, as previously attempted by SNL (Ref. 11), and flow lines should be pursued. Forensic work to reduce the uncertainty related to the water injection information should also be pursued. The accuracy of modeling the accident beyond {42:38} and predicting the amount of core degradation and final state are limited by the uncertainties in the water injection.

There are a number of additional areas where modeling could be improved. Information from TEPCO could be used to more accurately model the core assemblies, including the power profile, material masses, radionuclide inventories, and so on. These core features have direct impact on the core melt progression, hydrogen generation, and radionuclide release. The failure points of containment must also be modeled in a manner that reflects the 1F3 containment and physical processes occurring. To our knowledge, no models have predicted containment failure in 1F3 on an a priori/phenomenological basis.

Modeling of the reactor building, ventilation system, and vent lines should reflect the 1F3 details and not Peach Bottom or another NPP. The reactor building modeling impacts the hydrogen distribution and deflagration potential, radionuclide transport, and transportation to 1F4. These are key phenomena and concerns during the accident that MELCOR is designed to analyze.

There are additional areas where MELCOR code refinements may be required in order to reproduce the accident progression at 1F3. One example may be BWR core degradation modeling. Much of the previous experimentation and model work has focused on pressurized water reactors (PWRs) (e.g., more than 40 PWR fuel bundle degradation experiments versus 9 BWR experiments³⁶). Another example may be the impact of seawater

on the accident progression, which is currently unknown and not accounted for in MELCOR.

Finally, we have spent much time reading reports, interacting with Japanese representatives, and conducting various analyses. Although the accident provides numerous opportunities to learn from the plant response from a technological point of view, the human element of this accident should be equally understood. Besides the plant hardware, the operators were faced with beyond-design-basis operation. The operator actions and observations are key in understanding and modeling the accident progression. The operator interviews provide a picture of the challenges faced and some of the heroic actions of the operators.^{14,22}

ACKNOWLEDGMENT

Development of the 1F3 MELCOR model was supported by the joint DOE-NE/NRC “Fukushima Daiichi Accident Study.” This manuscript has been authored by UT-Battelle, LLC, under contract DE-AC05-00OR22725 with the DOE.

REFERENCES

1. L. J. OTT, “Advanced Severe Accident Response Models for BWR Application,” *Nucl. Eng. Des.*, **115**, 289 (1989); [http://dx.doi.org/10.1016/0029-5493\(89\)90054-X](http://dx.doi.org/10.1016/0029-5493(89)90054-X).
2. I. K. MADNI, “MELCOR Simulation of Long-Term Station Blackout at Peach Bottom,” presented at Water Reactor Safety Research Information Mtg, Gaithersburg, Maryland, October 22–24, 1990.
3. J. J. CARBAJO, “Severe Accident Source Term Characteristics for Selected Peach Bottom Sequences Predicted by the MELCOR Code,” NUREG/CR-5942, Oak Ridge National Laboratory (July 1993).
4. M. W. FRANCIS, “Long-Term Station Blackout Sequence and Mitigation MELCOR Model,” MS Thesis, University of Tennessee, Knoxville (May 2006).
5. D. H. COOK et al., “Station Blackout at Browns Ferry Unit One—Accident Sequence Analysis,” NUREG/CR-2182, Vol. I, ORNL/NUREG/TM-455/VI, Oak Ridge National Laboratory (Nov. 1981).
6. L. J. OTT, C. F. WEBER, and C. R. HYMAN, “Station Blackout Calculations for Browns Ferry,” presented at Water Reactor Safety Research Information Mtg, Gaithersburg, Maryland, October 22, 1985.
7. S. A. HODGE and L. J. OTT, “BWRSAR Calculations of Reactor Vessel Debris Pours for Peach Bottom Short-Term Station Blackout,” *Nucl. Eng. Des.*, **121**, 327 (1990); [http://dx.doi.org/10.1016/0029-5493\(90\)90015-P](http://dx.doi.org/10.1016/0029-5493(90)90015-P).
8. I. K. MADNI, “Analysis of Long-Term Station Blackout Without Automatic Depressurization at Peach Bottom Using MELCOR (Version 1.8),” NUREG/CR-5850, BNL-NUREG-52319, Brookhaven National Laboratory (May 1994).
9. S. BURNS to L. J. OTT, Personal Communication (Apr. 9, 2011).
10. L. J. OTT to J. L. BINDER, Personal Communication (Apr. 5, 2011).
11. R. O. GAUNTT et al., “Fukushima Daiichi Accident Study (Status as of April 2012),” SAND2012-6173, Sandia National Laboratories (July 2012).
12. “Report of Japanese Government to the IAEA Ministerial Conference on Nuclear Safety—The Accident at TEPCO’s Fukushima Nuclear Power Stations,” Nuclear Emergency Response Headquarters, Government of Japan (June 2011).
13. “Additional Report of Japanese Government to the IAEA—The Accident at TEPCO’s Fukushima Nuclear Power Stations (Second Report),” Nuclear Emergency Response Headquarters, Government of Japan (Sep. 2011).
14. “Results of Our Investigation of the Accidents and Subsequent Development at Fukushima Daiichi Nuclear Power Station,” Tokyo Electric Power Company Press Release (Dec. 22, 2011) (submitted to Japan Nuclear Energy Safety Organization).
15. “IAEA International Fact Finding Expert Mission of the Fukushima Dai-ichi NPP Accident Following the Great East Japan Earthquake and Tsunami,” International Atomic Energy Agency, Division of Nuclear Installation Safety (May 24–June 2, 2011).
16. “Review of Accident at Tokyo Electric Power Company Incorporated’s Fukushima Daiichi Nuclear Power Station and Proposed Countermeasures (Draft),” Japan Nuclear Technology Institute (Oct. 2011).
17. “Special Report on the Nuclear Accident at the Fukushima Daiichi Nuclear Power Station,” Rev. 0, INPO 11-005, Institute of Nuclear Power Operators (Nov. 2011).
18. “Fukushima Daiichi: ANS Committee Report,” American Nuclear Society Special Committee on Fukushima (Mar. 2012).
19. “Technical Knowledge of the Accident at Fukushima Daiichi Nuclear Power Station of Tokyo Electric Power Co., Inc. (Provisional Translation),” Nuclear and Industrial Safety Agency (Mar. 2012).
20. “The Official Report of the Fukushima Nuclear Accident Independent Investigation Commission, Executive Summary,” The Fukushima Nuclear Accident Independent Investigation Commission, The National Diet of Japan (July 2012).
21. R. O. GAUNTT et al., “MELCOR Computer Code Manuals—Reference Manuals Version 1.8.5,” NUREG/CR-6619, Rev. 2, SAND2000-2417/1, Sandia National Laboratories (Dec. 2000).
22. “Measures Taken at Fukushima Daiichi Nuclear Power Station and Fukushima Daini Nuclear Power Station (December 2011 Edition) List of Documents,” Tokyo Electric Power Company Press Release (Dec. 22, 2011).
23. “Unit 3, 4 Shift Supervisor Task Handover Journal,” English translation; http://www.tepco.co.jp/en/nu/fukushima-np/plant-data/f1_4_Nisshi3_4.pdf (accessed Dec. 1, 2011).

24. "State-of-the-Art Reactor Consequence Analyses Project, Volume 1: Peach Bottom Integrated Analysis," NUREG/CR-7110, Vol. 1, Sandia National Laboratories (Jan. 2012).
25. "Fukushima Daiichi Nuclear Power Station Unit 3 Parameters of Water Level and Pressure," Tokyo Electric Power Company (Dec. 1, 2011).
26. "Fukushima Daiichi Nuclear Power Station Unit 3 Parameters of Temperature," Tokyo Electric Power Company (Dec. 1, 2011).
27. "Preliminary Survey in Torus Room of Units 2 and 3, Fukushima Daiichi NPS," Photo and Videos Library, Tokyo Electric Power Company (Mar. 14, 2012).
28. "Fukushima Daiichi Nuclear Power Station Unit 3 Reactor Building First Floor TIP Room Environment Investigation Result (May 23, 2012)," Photo and Videos Library, Tokyo Electric Power Company (May 23, 2012).
29. "Result of Water Level Measurement at Unit 2-3 Torus Room of Fukushima Daiichi Nuclear Power Station," Photo and Videos Library, Tokyo Electric Power Company (June 7, 2012).
30. D. H. COOK, "Pressure Suppression Pool Thermal Mixing," NUREG/CR-3471, ORNL/TM-8906, Oak Ridge National Laboratory (Oct. 1984).
31. "Volume of Water Injected into the Reactor of Unit 1 to Unit 3 of Fukushima Nuclear Power Station," Tokyo Electric Power Company (May 31, 2011).
32. ANSI/ANS 5.1-1979, "Decay Heat Power in Light Water Reactors," American Nuclear Society, La Grange Park, Illinois (Aug. 1979).
33. A. G. CROFF, "ORIGEN2—A Revised and Updated Version of the Oak Ridge Isotope Generation and Depletion Code," ORNL-5621, Oak Ridge National Laboratory (July 1980).
34. S. R. GREENE, "Role of BWR Secondary Containments in Severe Accident Mitigation: Issues and Insights from Recent Analyses," presented at Workshop on Containment Integrity, Arlington, Virginia, June 14, 1988.
35. "Radiation Dose Measured in the Fukushima Daiichi Nuclear Power Station," Tokyo Electric Power Company; <http://www.tepco.co.jp/en/nu/fukushima-np/fl/data/2011/index-e.html> (accessed April 10, 2012).
36. J. REMPE et al., "Revisiting Insights from Three Mile Island Unit 2 Postaccident Examinations and Evaluations in View of the Fukushima Daiichi Accident," *Nucl. Sci. Eng.*, **172**, 223 (2012).